

Effects of the sample clock of digital-output MEMS accelerometers on vibration amplitude and phase measurements

Wan-Sup Cheung

Korea Research Institute of Standards and Science (KRISS), Daejeon, Republic of Korea

E-mail: wansup@kriss.re.kr

Received 14 August 2019, revised 9 October 2019

Accepted for publication 6 November 2019

Published 23 January 2020



Abstract

This paper presents the experimental results that when 100 seconds of vibration were recorded by the digital-output (DO) MEMS accelerometer with the 0.04% frequency-shifted sample clock, 23.8% of amplitude distortion with 71.2° of phase shift and 6.3% of amplitude distortion with 35.6° of phase shift were respectively observed in 10 Hz and 5 Hz of calibration frequencies. Theoretic models are also presented for the observed amplitude distortion and the phase shift caused by the frequency shift of the sample clock. Using the best-fitted frequency shift model by the least squares method, the vibration signals that were incorrectly sampled with the DO MEMS accelerometer were resampled at the corrected time slots and the corrected results showed the improvement of the measurement uncertainties in the amplitude and the phase of vibration within the 0.1% and 0.1° , respectively.

Keywords: digital-output accelerometer, MEMS accelerometer, vibration measurement, vibration calibration

(Some figures may appear in colour only in the online journal)

1. Introduction

Most of MEMS accelerometers, massively used in the industrial sectors of smart mobiles, automotive and unmanned vehicles, are designed to output digital measurements via the 4-wire SPI (serial peripheral interface) and/or two-wire I2C (inter-integrated circuit) interfaces. Those digital-output (DO) measurements are directly accessible to the 32 or 64-bit CPU of mobiles or automotive control units, without the additional circuits of analogue signal conditioners and AD converters. The small-sized and low-cost DO accelerometers have led to the explosive market expansion in aid of their easy interface to modern application processors. This trend will keep going in the emerging 5G markets and IoT products in the near future.

In this decade, three key comparisons [1–3] had been carried out to establish the traceability of vibration calibration and measurement between National Metrology Institutes (NMIs). The international comparisons were limited only to the analogue-output (AO) vibration pickups. Whilst AO vibration pickups are supported for the sensitivity calibration

according to the legacy vibration calibration standards (ISO 16063-1, 16063-11, 16063-15, and 16063-21), no calibration service for DO vibration sensors is available from NMIs. The reason may come from a technical limit of replacing the time series of digitally converted AO measurements by those of DO accelerometer measurements. A standard way of their replacement is not reported in the vibration metrology.

In section 2, a hybrid calibration setup under development in KRISS is introduced. In section 3, evaluation models of the vibration amplitude and phase components from the time series of DO accelerometer measurements and their corresponding standard uncertainties are described. The abnormal vibration measurements from the DO accelerometer are addressed. In section 4, a theoretic model is proposed to explain what causes the abnormal vibration measurements. From the model is derived the prediction models of the vibration amplitude distortion and the biased phase shift caused by the inexact sampling clock. In section 5, the resample method is proposed and then examined to evaluate the achievable standard uncertainties. Furthermore, the user-supplied

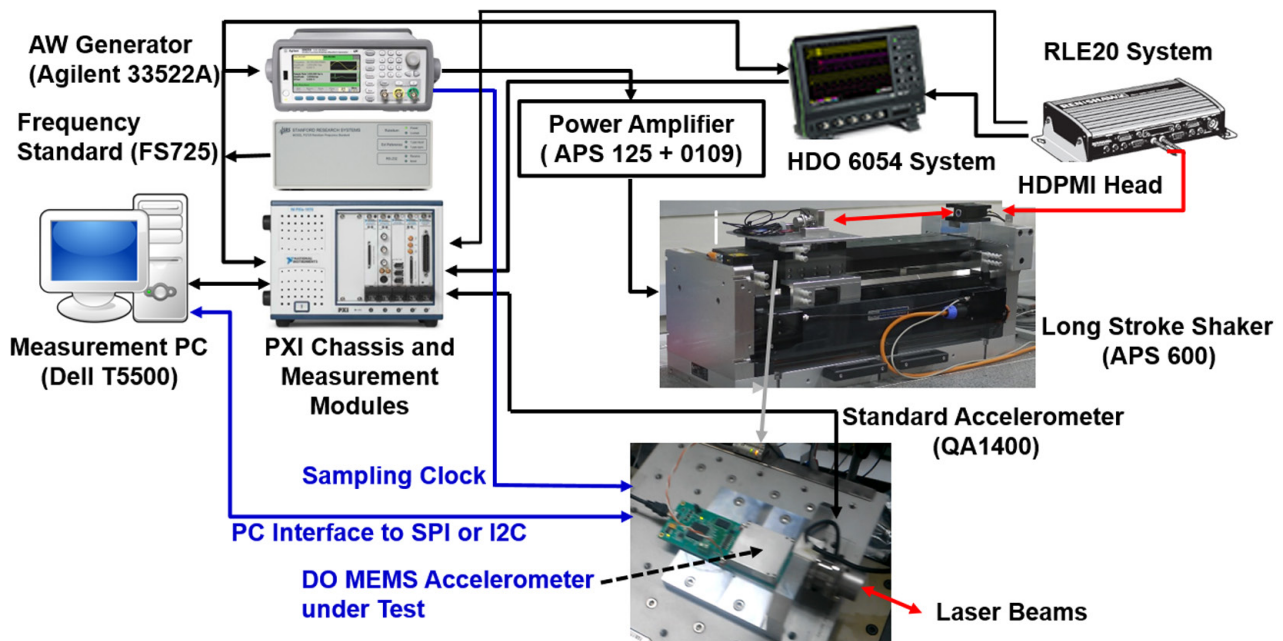


Figure 1. Hybrid (analogue and digital output integrated) linear vibration calibration system.

external sample scheme, independent of the low-cost and inexact internal clock of the DO accelerometer, is also tested to evaluate them. Finally concluding remarks are summarised.

2. Hybrid calibration setup for AO and DO vibration pickups

KRISS had decided to add a new real-time data acquisition unit for DO vibration sensors to the legacy vibration calibration systems limited to the AO vibration pickups. Figure 1 shows a new linear vibration calibration system under development. It does not only fulfil all the requisites for the legacy AO vibration calibration system but also presents real-time communication with DO accelerometers. It is referred to as the ‘hybrid (analogue- and DO integrated)’ calibration system. In figure 1, the signal chains connected by the black solid lines indicate the analogue signals for the legacy primary vibration calibration system, the blue solid lines do the digital signal lines connected to the DO vibration sensors under calibration, and the red solid lines do the optic paths of the laser interferometer. Most makers of DO MEMS accelerometers provide their own evaluation kits. Whenever the evaluation kits do not provide an input port for the user-supplied external sample clock, they are not well fitted with the KRISS vibration calibration system since the synchronisation of the sample clock of the vibration calibration system with that of the DO MEMS sensor is not feasible. As shown in figure 1, the KRISS vibration calibration system exploits the calibrated frequency standard (model SF725) of 0.1 ppb (or less) to stabilise the time bases of all instruments with the external reference clock input. Unlike the stabilised and synchronised instruments in the KRISS calibration system, most MEMS accelerometers and gyroscopes use a low-cost internal oscillator with the frequency stability of several hundred ppm (or more). Effects of

the inexact internal sample clock on the calibration results of the DO vibration sensors are not studied systematically. More specifically, the internal sample clock is not certainly reported to make no effect on the vibration measurement uncertainty of DO MEMS accelerometers or gyroscopes.

The DO MEMS inertial measurement unit (IMU) of model ADIS 16488B was selected to examine the effects of the internal sample clock on vibration measurements. As shown in figure 1, the DO IMU model (ADIS 16448B) under calibration is fixed on the dedicated evaluation board (EVAL-ADIS), which enables real-time acquisition of the 3-axis acceleration and 3-axis angular velocity, including the 3-axis magnetic field strength and ambient pressure, through the USB-to-SPI interface and communication software (version 1.14.3.4545). The IMU evaluation board is fixed rigidly on the vibration table of the long stroke vibration shaker (APS 600).

The first channel of the dual channel waveform generator (Agilent 33522A) is used to supply a sine function to the power amplifier (APS 126 + APS 0109), which supplies desired current to the long stroke vibration shaker. The frequency stability of the waveform generator is kept within the level of 0.1 ppb (or less) since it receives the 10 MHz reference clock from the frequency standard (FS 725) and synchronises its own internal clock to it. The second channel of the waveform generator (Agilent 33522A) is programmed to supply the external sample clock to the DO MEMS sensor. The 32-bit position counter (PXIe 6612) and the 24-bit AD converter module (PXI 5922) are operated by the stabilised time base provided by the 100 MHz bus clock of the chassis frame (PXIe 1062Q) synchronised with the 10 MHz frequency standard (FS 725). The up-down position counter (PXIe 6612) measures vibration displacement from the laser encoder signals of the RLE 20 laser interferometer. The flexible 24-bit AD converter (PXI 5922) converts the analogue voltage signal

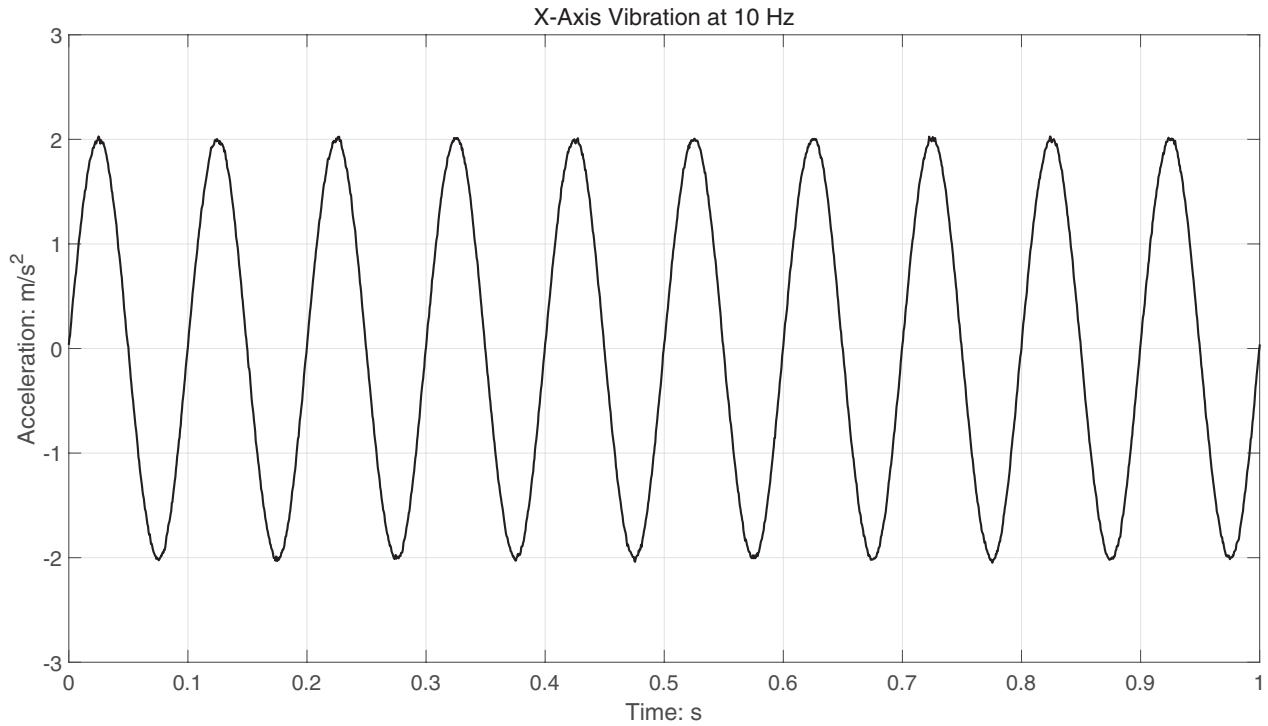


Figure 2. 10 Hz vibration signal measured from the DO MEMS IMU model (ADIS 16488B).

from the working standard accelerometer (QA 1400) into the binary data and transfers them to the measurement PC (Dell T5500) in the real time.

3. Measured vibration amplitude and phase from DO accelerometers and standard uncertainties

As guided in ISO 16063-11 (1999), a simple harmonic motion is used to calibrate the sensitivity of a vibration pickup. The measured vibration signal $v(n\Delta\tau)$ from the DO vibration sensor each sample interval $\Delta\tau$ are described as

$$v(n\Delta\tau); n = 1, 2, \dots, N_p \times M. \tag{1}$$

N_p indicates the number of samples per period and M does the number of periods.

Figure 2 illustrates the 10 Hz vibration signal measured from the x -axis DO accelerometer of the MEMS IMU model (ADIS 16488B). It looks closely similar to the vibration signal measured from the AO accelerometer, i.e. the working standard accelerometer (QA 1400). Actual vibration measurement using the DO MEMS sensor is much simpler than the analogue vibration measurement that requires a series of analogue and digital instruments (analogue signal amplifiers, anti-aliasing filters, precision AD converters, and the real-time high-speed data communication unit).

Given the recorded signals during M periods, the m th Fourier cosine and sine components corresponding to period m ($m = 1, \dots, M$) are evaluated as follows:

$$C(m) = \frac{2}{N_p} \sum_{n=1}^{N_p} v(((m-1)N_p + n)\Delta\tau) \cdot \cos\left(\frac{2\pi n}{N_p}\right) \tag{2}$$

$$S(m) = \frac{2}{N_p} \sum_{n=1}^{N_p} v(((m-1)N_p + n)\Delta\tau) \cdot \sin\left(\frac{2\pi n}{N_p}\right).$$

The averaged Fourier cosine and sine coefficients are readily obtained as

$$C_M = \frac{1}{M} \sum_{m=1}^M C(m), \quad S_M = \frac{1}{M} \sum_{m=1}^M S(m) \tag{3}$$

The vibration amplitude and phase of the recorded signals during M periods are evaluated as

$$A = \sqrt{C_M^2 + S_M^2}, \quad \varphi = \tan^{-1}\left(\frac{-S_M}{C_M}\right). \tag{4}$$

The standard uncertainties of the vibration amplitude A and phase φ in equation (4) are evaluated as

$$u_r^2(A) = \frac{u^2(A)}{A^2} = \frac{C_M^2}{(C_M^2 + S_M^2)^2} u^2(C_M) + \frac{S_M^2}{(C_M^2 + S_M^2)^2} u^2(S_M) + \frac{2C_M S_M}{(C_M^2 + S_M^2)^2} u(C_M, S_M) \tag{5}$$

and

$$u^2(\varphi) = \frac{S_M^2}{(C_M^2 + S_M^2)^2} u^2(C_M) + \frac{C_M^2}{(C_M^2 + S_M^2)^2} u^2(S_M) - \frac{2C_M S_M}{(C_M^2 + S_M^2)^2} u(C_M, S_M). \tag{6}$$

$u_r(A)$ denotes the relative standard uncertainty of the estimated amplitude and $u_r(\varphi)$ that of the estimated phase. $u(C_M)$ and $u(S_M)$ indicate the standard uncertainties of the averaged Fourier cosine and sine coefficients and $u(C_M, S_M)$ the covariance of M cosine and sine components divided by the number of periods (M). In summary, equations (1) through (6) describe detailed computation schemes of estimating the vibration amplitude and phase and their corresponding standard uncertainties.

The vibration signal shown in figure 1 was acquired in the internal sample clock mode of the DO IMU model (ADIS

Table 1. Measured relative amplitudes and phases and their corresponding standard uncertainties at the four calibration frequencies of 1 Hz, 2 Hz, 5 Hz, and 10 Hz.

Calibration frequency	Internal clock sample mode			
	Measured vibration		Standard uncertainty	
	Amplitude	Phase	Amplitude	Phase
Hz	Relative	°	%	°
10	0.762	−159.7	27.0	46.2
5	0.937	−125.5	6.0	21.1
2	0.990	−103.7	0.9	8.2
1	0.997	−95.9	0.3	4.1

16488B), whose configured sample rate was 2.46 kHz. A fixed record length of 246,000 samples (equivalent to the recording time of 100 s) was selected in this work. The applied sinusoidal acceleration amplitudes were finely tuned to 2.0 m s^{-2} for the calibration frequency range of 2 Hz through 10 Hz and 1.0 m s^{-2} for the 1 Hz calibration frequency.

The measured relative amplitudes and phases at the four calibration frequencies and their corresponding standard uncertainties are listed in table 1. The relative amplitudes indicate the ratio of the measured amplitudes to the applied acceleration amplitudes. At the 10 Hz and 5 Hz frequencies, they were observed to be 76.2% and 93.7% of the applied acceleration level. As listed in the 4th and 5th columns of table 1, the standard uncertainties of the amplitudes and phases for the four frequencies were too high to be regarded as acceptable measurements because they excessively exceed the quality control limits of the 0.1% amplitude and 0.2° phase bounds. To the contrary of the abnormal standard uncertainties of the DO accelerometer, those of the analogue standard accelerometer (QA 1400) were observed to be within the quality control limits.

As listed in table 1, the phase standard uncertainties were observed abnormally high. They were the first unexpected results from the DO MEMS accelerometer. Several attempts had been made to inspect underlying causes behind the unexpected results. Specifically, it took quite a long time to experimentally confirm that there was no missed sample during the acquisition of the digital outputs of the ADIS 16488B model. It confirmed that the newly added real-time data communication (acquisition) unit for DO vibration sensors works properly. Resultantly, main attempts had focused on the vibration measurement principles of the DO accelerometer specified in the ADIS 16488B data sheet.

4. Effects of an inexact internal sample clock on amplitude and phase measurements

A critical clue on the abnormal vibration measurements listed in table 1 was observed from the plot of the evaluated vibration amplitudes and phases over the 999 periods of 10 Hz

vibration, as shown in figure 3. The amplitude and phase each period was evaluated from the paired Fourier cosine and sine components described in equation (2). Whilst the vibration amplitudes were kept within a tight level of 0.1%, the continuously varied phases were observed over the whole periods.

The initial phase at the first period was -88.6° and the final one at the last period was -230.9° . The total phase difference was -142.3° and the mid phase was -159.7° , which equals the measured phase given in the 10 Hz calibration frequency of table 1. The linearly varied phases over the whole periods have been never observed from the legacy AO vibration accelerometers under calibration. At the beginning of this work, it was the second unexpected result observed from the DO MEMS accelerometer. It was certain that such linearly varied phases over the whole periods lead serious amplitude distortion and phase shift, such as the 27% amplitude and 46.2° phase standard uncertainties at the 10 Hz calibration frequency of table 1.

An infinitesimal phase shift of -0.142° per period ($-142.3^\circ/999$ periods) was observed to occur continuously. It can be observed if the actual sample rate of the DO MEMS IMU model is infinitesimally shifted from the nominal frequency of 2.46 kHz in the technical datasheet. Such sample frequency shift inevitably comes from the low-cost and inexact internal sample clock (directly related to the local oscillator of the DO IMU model). The frequency of a simple harmonic vibration measured by the DO IMU model is also shifted such that it differs from the reference frequency generated by the arbitrary waveform generator (Agilent 33522A). The vibration signal measured by the DO IMU model at the reference time t (synchronised to the frequency standard (SF 725)) is modelled as

$$v(t) = A \cos(2\pi f(1 + \delta)t + \varphi). \quad (7)$$

The symbol δ denotes a relative frequency shift of calibration frequency f caused by the inexact (frequency-shifted) internal sample clock of the DO accelerometer. Equation (7) shows that the infinitesimal phase shift $2\pi\delta$ after one period is added to the initial phase φ . The relative frequency shift δ of the DO accelerometer obviously causes the phase shift $2\pi\delta$ every period.

The Fourier cosine and sine coefficients of equation (7) for the m -th period are given as

$$\begin{aligned} C_m(f) &= \frac{2}{T} \int_{(m-1)T}^{mT} v(t) \cdot \cos(2\pi ft) dt \\ &= A \frac{\sin(\pi\delta)}{\pi\delta} \cos(2\pi\delta \cdot m + \varphi - \pi\delta) \left(1 + \frac{\delta}{2} \left(1 + \frac{\delta}{2}\right)^{-1}\right) \\ &\cong A \frac{\sin(\pi\delta)}{\pi\delta} \cos(2\pi\delta \cdot m + \varphi - \pi\delta) \end{aligned} \quad (8)$$

and

$$\begin{aligned} S_m(f) &= \frac{2}{T} \int_{(m-1)T}^{mT} v(t) \cdot \sin(2\pi ft) dt \\ &= A \frac{\sin(\pi\delta)}{\pi\delta} \sin(2\pi\delta \cdot m + \varphi - \pi\delta) \left(-1 + \frac{\delta}{2} \left(1 + \frac{\delta}{2}\right)^{-1}\right) \\ &\cong -A \frac{\sin(\pi\delta)}{\pi\delta} \sin(2\pi\delta \cdot m + \varphi - \pi\delta). \end{aligned} \quad (9)$$

The symbol T ($T = 1/f$) is the period of calibration frequency. Since the relative frequency shift δ of the DO accelerometer is

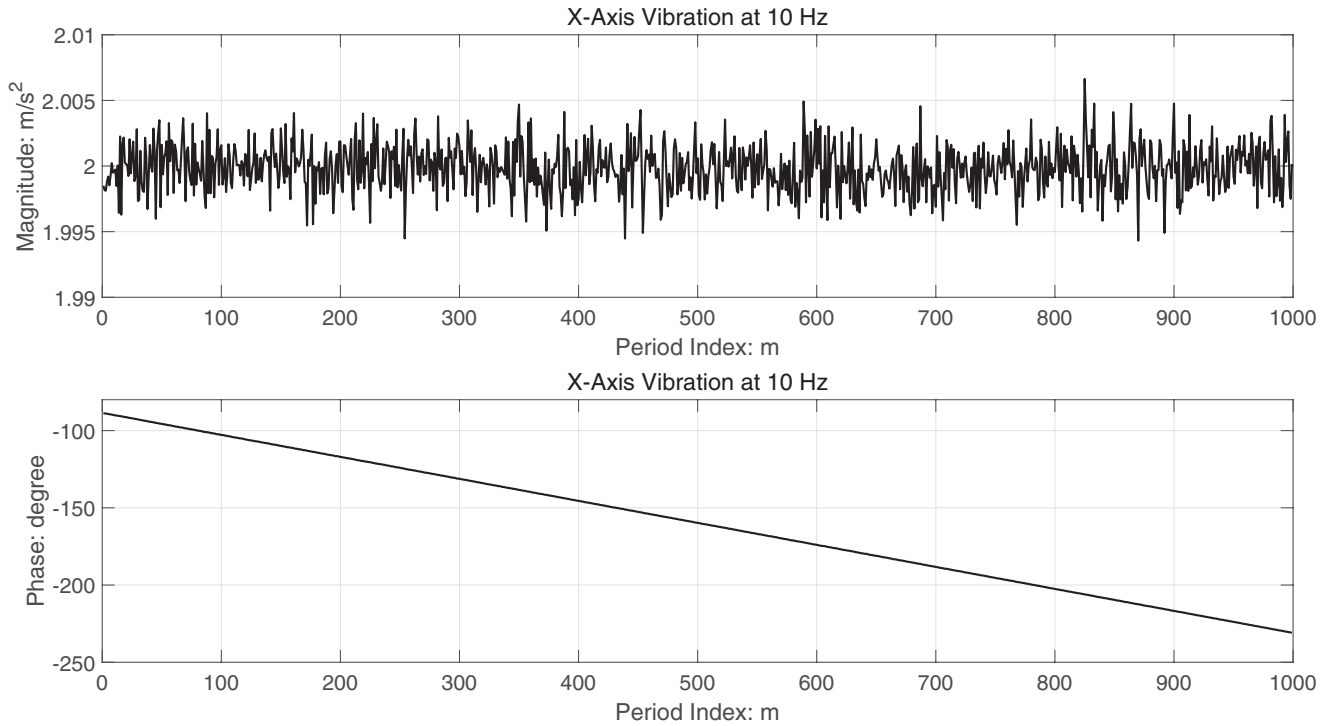


Figure 3. Amplitudes and phases measured in the internal sample clock mode during the 999 periods of 10 Hz vibration.

Table 2. Estimated relative frequency shifts at the four calibration frequencies of 1 Hz, 2 Hz, 5 Hz, and 10 Hz.

Calibration frequency	Periods	Relative frequency shift	Biased initial phase
Hz	M	$\delta \times 10^4$	$\varphi + \pi\delta$
10	999	-3.958	-88.6°
5	499	-3.957	-90.0°
2	199	-3.960	-89.6°
1	99	-3.963	-88.9°

in the range of hundreds of ppm (or less), the Fourier cosine and sine coefficients in equations (8) and (9) are approximated as

$$\begin{aligned} \frac{A_m}{A} &= \frac{1}{A} \sqrt{C_m(f)^2 + S_m(f)^2} \\ &\cong \frac{\sin(\pi\delta)}{\pi\delta} = \text{sinc}(\pi\delta) \\ \varphi_m &= \tan^{-1} \left(\frac{-S_m(f)}{C_m(f)} \right) = 2\pi\delta \cdot m - \pi\delta + \varphi. \end{aligned} \quad (10)$$

Equation (10) unfolds that the relative frequency shift δ of the internal sample clock leads to the amplitude distortion of sinc-function $\text{sinc}(\pi\delta)$ and the extra phase bias of $(2\pi\delta \cdot m - \pi\delta)$. Specifically, the linear phase model of equation (10) matches well with the measured phases shown in figure 3. The biased phase shift of $2\pi\delta$ is added after one period such that an accumulated phase shift after m periods equals $2\pi\delta \cdot m - \pi\delta$. The initial phase ($m = 1$) is $\varphi + \pi\delta$, i.e. the initial phase biased by $\pi\delta$. They mean that a DO accelerometer with an inexact (frequency-shifted) internal sample clock presents ‘distorted and biased’ information about the vibration amplitude and phase. Equation (10) describes theoretically the quantitative effects of the relative frequency shifted sample clock of the DO accelerometer on the amplitude and phase measurements.

It becomes apparent that digitally converted analogue vibration signals, similar to the output streams of the DO accelerometer, are also not free from the effects of the frequency-shifted (or inexact) sample clock of the selected AD converter. The sample clock accuracy must be one of systematic problems imbed not only in the DO vibration sensors with a low-cost and inaccurate internal clock but also in the vibration signals sampled by the local clock-based AD converters. It should be noted that acceptable vibration amplitude and phase measurements are not achievable without the tight control of the sample clock for both the AD converter for analogue vibration pickups and the DO accelerometers. It is the reason that the vibration calibration system shown in figure 1 adopts the 10 MHz reference clock of the frequency standard (FS 725).

4.1. Estimation scheme for the relative frequency shift

An effective way of estimating the relative frequency shift δ is considered in this section. The phases in equation (10) evaluated each period are rewritten as a linear model

$$\begin{aligned} \varphi_m &= 2\pi\delta \cdot (m - 1) + \varphi_1 \quad (m = 1, \dots, M) \\ \varphi_1 &= \varphi + \pi\delta. \end{aligned} \quad (11)$$

The symbol φ_1 denotes the initial phase ($m = 1$). Given the M measured phases $\{\varphi_m; \text{ for } m = 1, \dots, M\}$, the best fitted parameters δ and φ_1 are readily estimated using the least squares method. Table 2 shows the estimated relative frequency shifts for the four calibration frequencies. The averaged relative frequency shift δ at the four calibration frequencies was -3.96×10^{-4} and its relative standard uncertainty was 0.034%.

It is interesting to understand the physical meaning of the estimated relative frequency shift δ , i.e. -3.96×10^{-4}

Table 3. Predicted vibration amplitude and phase from the estimated relative frequency shift.

Calibration frequency	Relative frequency shift	Distorted amplitude ratio	Biased phase shift	Initial phase
Hz	$\delta \times 10^4$	$\text{sinc}(M \cdot \pi\delta)$	$M \cdot \pi\delta$	φ
10	-3.96	0.762	-71.2°	-88.5°
5		0.937	-35.6°	-89.9°
2		0.990	-14.2°	-89.5°
1		0.998	-7.1°	-88.8°

in table 2. A negative sign indicates that the internal sample clock of the DO accelerometer is faster than the reference one such that the phase angle of the measured vibration signal is delayed relatively by $2\pi\delta$ after one period (N_p samples later). It thus indicates that the internal sample time of the DO accelerometer is slightly faster by 0.04% than the reference one. Oppositely, a positive sign indicates that the internal sample clock is slower than the reference one such that the phase angle of the measured vibration signal leads relatively by $2\pi\delta$ after one period. Resultantly, the estimated frequency shift does not allow for us to know the actual sample times of the DO accelerometer but also to resample the time series of ‘interpolated’ measurements at the corrected sample times from the recorded signals in the inexact sample times. This resample scheme will be further examined in section 5.

4.2. Prediction models of distorted amplitude and biased phase

Prediction models of the distorted amplitude and the biased phase, caused by the inexact internal sample clock of the DO accelerometer, are described in this section. To derive the prediction models, the proposed relative frequency model of equation (7) is exploited. From equations (8) and (9), the averaged Fourier cosine and sine components over the M periods are obtained by selecting the integration range from zero to the M periods (MT). Equations (12) and (13) describe the averaged Fourier cosine and sine components over the M periods.

$$\begin{aligned}
 C(f) &= \frac{2}{MT} \int_0^{MT} v(t) \cdot \cos(2\pi ft) dt \\
 &= A \frac{\sin(M \cdot \pi\delta)}{M \cdot \pi\delta} \cos(M \cdot \pi\delta + \varphi) \times \left\{ 1 + \frac{\delta}{2} \left(1 + \frac{\delta}{2} \right)^{-1} \right\} \\
 &\cong A \frac{\sin(M \cdot \pi\delta)}{M \cdot \pi\delta} \cos(M \cdot \pi\delta + \varphi) \text{ for } \left(\frac{\delta}{2} \right) \ll 1, \quad (12)
 \end{aligned}$$

and

$$\begin{aligned}
 S(f) &= \frac{2}{MT} \int_0^{MT} v(t) \cdot \sin(2\pi ft) dt \\
 &= -A \frac{\sin(M \cdot \pi\delta)}{M \cdot \pi\delta} \sin(M \cdot \pi\delta + \varphi) \times \left\{ 1 - \frac{\delta}{2} \left(1 + \frac{\delta}{2} \right)^{-1} \right\} \\
 &\cong -A \frac{\sin(M \cdot \pi\delta)}{M \cdot \pi\delta} \sin(M \cdot \pi\delta + \varphi) \text{ for } \left(\frac{\delta}{2} \right) \ll 1. \quad (13)
 \end{aligned}$$

Finally, the averaged amplitude and phase A_M and φ_M over the M periods are evaluated as

$$\begin{aligned}
 \frac{A_M}{A} &= \frac{1}{A} \sqrt{C(f)^2 + S(f)^2} \\
 &\cong \frac{\sin(M \cdot \pi\delta)}{M \cdot \pi\delta} = \text{sinc}(M \cdot \pi\delta) \\
 \varphi_M &= \tan^{-1} \left(\frac{-S(f)}{C(f)} \right) \cong M \cdot \pi\delta + \varphi. \quad (14)
 \end{aligned}$$

Table 4. Distorted amplitudes and biased phases caused by the internal sample clock accuracy of the DO accelerometer.

Number of periods	Internal clock accuracy	Distorted amplitude ratio	Biased phase shift
M	δ ppm	$1 - \text{sinc}(M \cdot \pi\delta)$ %	$M \cdot \pi\delta$ °
100	500	0.41	9.00
	100	0.02	1.80
	50	0.004	0.90
	10	0.0002	0.18
	5	0.00004	0.09

Equation (14) explains that the relative frequency shift δ of the sample clock of the DO sensor leads to the amplitude distortion of sinc-function $\text{sinc}(M \cdot \pi\delta)$ and the extra biased phase shift of $M \cdot \pi\delta$ in addition to the initial phase φ . Table 3 illustrates the calculated amplitudes and phases using equation (14) for the four calibration frequencies.

The 3rd column of table 3 indicates the relative amplitude ratios of the calculated amplitude to the applied acceleration level. The distorted amplitude ratios in table 3 are found to equal the measured vibration amplitudes in the 2nd column of table 1. The averaged phase in equation (14) is equal to a sum of the biased phase shift $M \cdot \pi\delta$ and the initial phase φ such that the sums (the sums of the 4th and 5th columns in table 3) are -159.7° , -125.5° , -103.7° -95.5° for the 10 Hz, 5 Hz, 2 Hz, and 1 Hz calibration frequencies, respectively. They actually equal the measured phases listed in the 3rd column of table 1. Resultantly, the calculated amplitude and phases for the 10 Hz, 5 Hz, 2 Hz, and 1 Hz calibration frequencies are found to match very well with the actually measured ones.

It is interesting to note that equation (14) can predict the distorted amplitude ratio and the biased phase shift due to the local clock accuracy of the DO accelerometer. Table 4 illustrates the predicted amplitude ratios and the biased phase shifts for the different sample clock accuracies from 500 ppm to 5 ppm.

The 100 periods ($M = 100$) were selected in table 4, which is regarded as the lower bound of actually selected periods for the vibration calibration. As previously commented for the quality control limits, the biased phase shifts for the internal clock accuracy of 500 ppm, 100 ppm and 50 ppm are rejected since they are out of the 0.2° phase bounds. The DO accelerometer with the internal clock accuracy equal to or less than 10 ppm can meet the 0.2° phase bounds. Unlike the biased phase shifts, the distorted amplitude ratio is seen to be less sensitive to the internal clock accuracy. The 500 ppm internal clock accuracy causes the 0.41% amplitude distortion. The 100 ppm (or better) internal clock accuracy of the DO accelerometer is found to present the 0.02% amplitude distortion. Resultantly, the internal sample clock accuracy of DO accelerometers is valuable for users to predict the achievable standard uncertainty. Most makers of DO accelerometers and gyroscopes, however, are reluctant to notify the sample clock accuracy in the specifications of the data sheet.

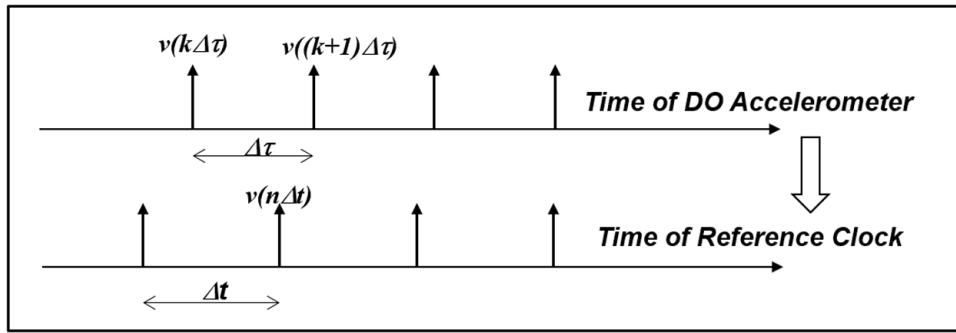


Figure 4. Resample scheme using two neighbouring measurements sampled at the local time of the DO sensor.

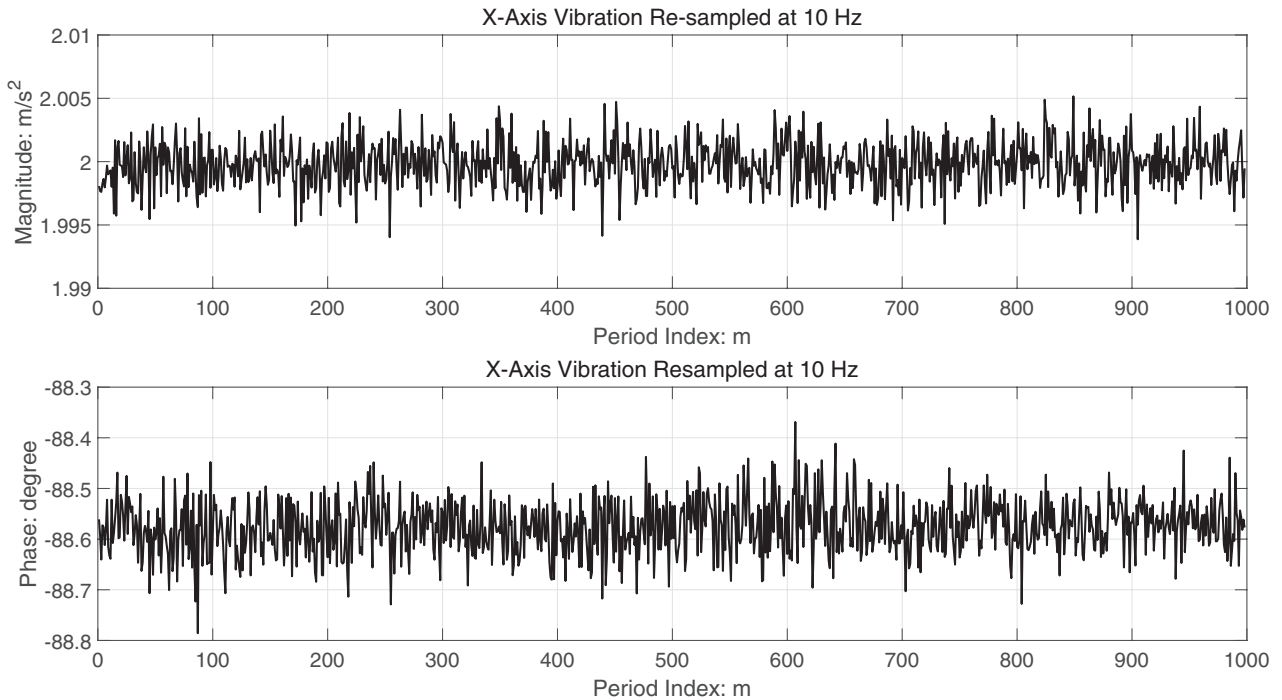


Figure 5. Amplitudes and phases evaluated from the resampled measurements at the corrected sample times.

5. Experimental results and discussions

In this section, a logical way is considered to resample a time series of ‘interpolated’ measurements at the corrected sample times from the sampled signals of the DO accelerometer at the incorrect sample times. The proposed resample scheme is examined to evaluate the achievable standard uncertainties. A hardwired ‘external sample’ scheme for acquiring the vibration measurements of the DO accelerometer is also considered, which is free from its own low-cost and and inaccurate internal oscillator. It is also examined to evaluate the achievable vibration amplitude and phase standard uncertainties.

5.1. Proposed resample scheme

In this work, the estimated relative frequency shift δ is exploited to calculate the actual sample times of the DO accelerometer. Chosen a simple harmonic motion of calibration frequency f , the measured phase angle from the DO accelerometer at the

Table 5. Evaluated vibration amplitudes and phases from the resampled signals at the corrected sample time.

Clairation frequency	Resample mode			
	Measured vibration		Standard uncertainty	
	Amplitude	Phase	Amplitude	Phase
Hz	Relative	°	%	°
10	1.000	-88.6	0.09	0.05
5	1.000	-89.9	0.05	0.04
2	1.000	-89.6	0.04	0.02
1	0.999	-88.9	0.06	0.03

k -th sample time $k\Delta\tau$ is defined as $(2\pi f \cdot k\Delta\tau + \varphi)$. It is actually identical to the sampled phase angle of equation (6) at the reference time $k\Delta t$, i.e. $(2\pi(1 + \delta)f \cdot k\Delta t + \varphi)$. The ratio of the actual sample time of the DO accelerometer to the reference sample time is given as

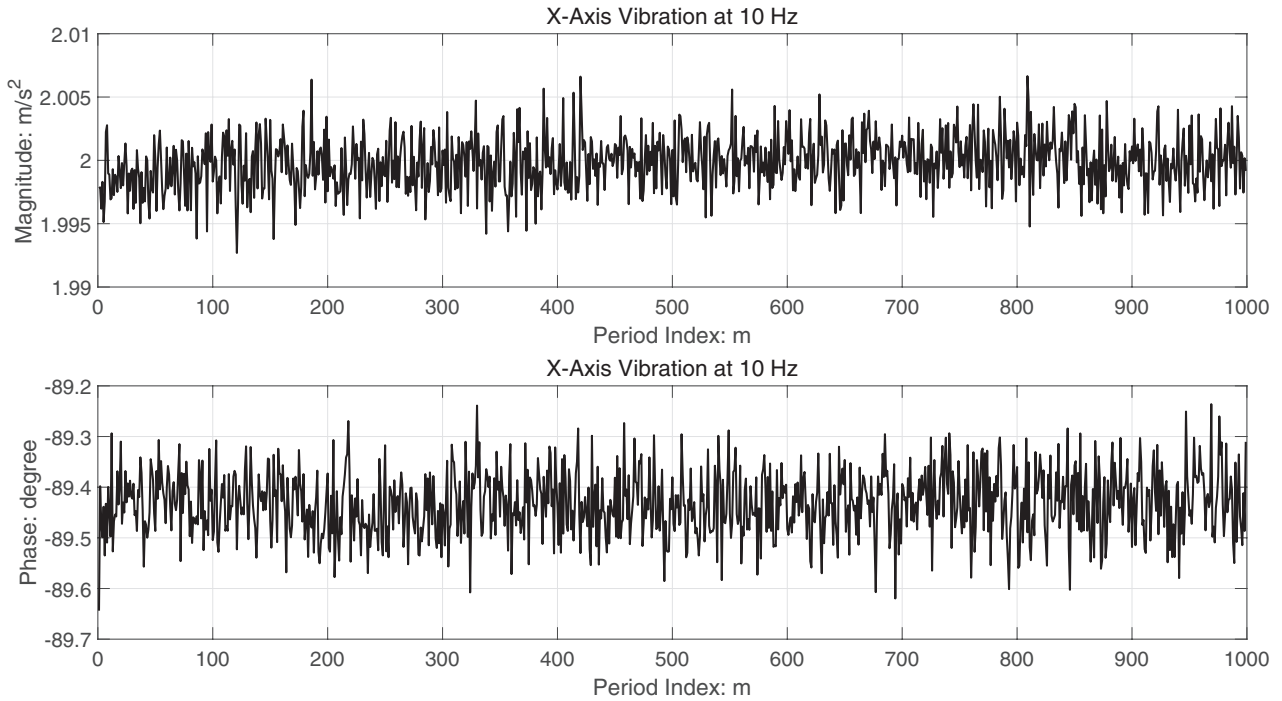


Figure 6. Amplitudes and phases measured in the external sample clock mode during 1000 periods of 10 Hz vibration.

$$\frac{\Delta\tau}{\Delta t} = 1 + \delta. \tag{15}$$

It means that the actual sample time of the DO sensor is biased by the relative frequency shift δ in comparison to the reference sample time. Resultantly, the actual sample time of the DO accelerometer was not Δt but $(1 + \delta)\Delta t$. Figure 4 illustrates a distinctive difference between the two sample times $\Delta\tau$ and Δt . The recorded signals in equation (1) were actually sampled every time $\Delta\tau = (1 + \delta)\Delta t$.

As shown in figure 4, a simple ‘linear interpolation’ scheme was used to resample the time signal $v(n\Delta t)$ at the reference (or corrected) sample time $n\Delta t$ from the two neighbouring recorded signals $v(k\Delta\tau)$ and $v((k + 1)\Delta\tau)$ sampled at the local times of the DO sensor. This resample scheme is readily implemented when the recorded signals and the relatively shift frequency are given (as previously shown in figure 2 and table 3). Figure 5 illustrates the vibration amplitudes and phases evaluated every period from the resampled measurements at the corrected sample times.

As shown in figure 5, the evaluated amplitudes and phases are satisfactory since they meet the quality control (0.1% amplitude and 0.2 ° phase) bounds. Table 5 lists the vibration amplitudes and phases evaluated from the resampled signals at the corrected sample time and their corresponding standard uncertainties.

Unlike the distorted amplitudes and biased phases and their standard uncertainties listed in table 1, table 5 reveals that the resample scheme improves them to the sufficiently acceptable level. It is interesting to note that the estimated relative frequency shift δ plays a significant role in improving the standard uncertainties. The proposed estimation scheme of the relative frequency shift δ seems to be one of the

Table 6. Vibration amplitudes and phases measured in the external sample clock mode.

Clairation frequency	External sample mode			
	Measured vibration		Standard uncertainty	
	Amplitude	Phase	Amplitude	Phase
Hz	Relative	°	%	°
10	1.000	−89.4	0.09	0.06
5	1.000	−89.9	0.08	0.03
2	1.000	−89.2	0.05	0.02
1	1.000	−89.9	0.06	0.03

effective calibration methods of the local oscillator of the DO MEMS sensors.

5.2. Use of external sample clock

At the beginning of this work, the DO MEMS IMU model (ADIS 16448B) was chosen since it supports the user-supplied external sample clock input port. The 2nd channel output of the waveform generator (Agilent 33522A) was programmed to generate the external sample clock of 2kHz (2k samples per second). As shown in figure 1, the external sample clock is supplied to the general purpose IO (GPIO) port of the DO IMU model. Once the measurement mode is started the digital outputs sampled by the external clock are transferred to the measurement PC in the same way as done in the internal sample clock mode.

As described in equations (1) through (6), the vibration amplitudes and phases every period were calculated and their

corresponding standard uncertainties were also evaluated. Figure 6 shows the amplitudes and phases measured in the external sample clock mode. The evaluated amplitudes and phases are seen to be very satisfactory.

Table 6 lists the vibration amplitudes and phases evaluated from the recorded signals in the external sample clock mode of the DO IMU model and their corresponding standard uncertainties. It indicates that the standard uncertainty of the vibration amplitude is less than 0.1% and that of the vibration phase is lower than 0.1° . The sufficiently acceptable standard uncertainties of the vibration amplitudes and phases are shown to be achieved in the external sample clock mode of the DO IMU model.

The external sample clock port seems to be extremely useful and effective for the calibration of DO accelerometers and gyroscopes. Such usefulness and effectiveness certainly encourages all the makers of DO MEMS accelerometers and gyroscopes to adopt the external sample clock port to their future products. Furthermore, the external sampling clock port makes DO MEMS sensors free from their own low-cost and inaccurate internal oscillators.

6. Concluding remarks

This work introduces a hybrid (analogue- and DO integrated) linear vibration calibration system, which is under development to provide new calibration and measurement services for the DO vibration sensors. The abnormal vibration amplitudes and phases measured from the DO accelerometer are addressed. They are theoretically proved to be caused by the inexact (frequency-shifted) internal sample clock of the DO accelerometer. The linear model of the relative frequency shift is proposed and the least squares method is tried to estimate the

model parameters. Furthermore, the proposed model enables analytic analysis for the effects of the inexact sample clock of the DO accelerometer on the vibration amplitude and phase measurements. The estimated relative frequency shift makes it possible to calculate the inexact sample times of the DO accelerometer. The resample scheme at the corrected sample times is shown to improve the vibration amplitude and phase standard uncertainties to the sufficiently acceptable level. The external sample clock mode of the DO accelerometer is also tested because it is free from the low-cost and inexact internal clock. It is also shown to present not only the sufficiently acceptable amplitude and phase measurements but also their satisfactory standard uncertainties inside the quality control bounds. Finally, all the makers of DO MEMS accelerometers and gyroscopes are encouraged to adopt the external sample clock port to their future products.

Acknowledgments

This work was supported by the KRISS major research project for the Center for Mechanical Metrology (project code 19011032).

References

- [1] Bruns T, Gripper G P and Taubner A 2014 Final report on the CIPM key comparison CCAUV.V-K2 *Metrologia* **51** 09002
- [2] Taubner A, Bruns T and Cheung W S 2014 Bilateral comparison in primary angular vibration calibration CCAUV.V-B1 *Metrologia* **51** 09006
- [3] Sun Q, Yang L, Bartoli C and Veldman I 2017 Final report of CCAUV.V-K3: key comparison in the field of acceleration on the complex voltage sensitivity *Metrologia* **54** 09001